Journal of Stored Products Research 65 (2016) 19–29

Contents lists available at ScienceDirect

Journal of Stored Products Research

journal homepage: www.elsevier.com/locate/jspr

Simulation of heating uniformity in a heating block system modified for controlled atmosphere treatments

Rongjun Yan [a], Zhi Huang [a], Hankun Zhu [a], Judy A. Johnson [b], Shaojin Wang [a, c, *]

[a] College of Mechanical and Electronic Engineering, Northwest A&F University, Yangling, Shaanxi 712100, China
[b] USDA-ARS, San Joaquin Valley Agricultural Sciences Center, 9611 S. Riverbend Avenue, Parlier, CA 93648, USA
[c] Department of Biological Systems Engineering, Washington State University, Pullman, WA 99164-6120, USA

ARTICLE INFO

Article history:
Received 9 October 2015
Received in revised form
15 November 2015
Accepted 15 November 2015
Available online xxx

Keywords:
Controlled atmosphere
Heating block system
Heating rate
Insects
Simulation
Temperature distribution

ABSTRACT

Reliable and repeatable insect thermal mortality data rely on the performance of a heating device. Computer simulation has been widely used to optimize structures, design parameters and process conditions. To improve the temperature uniformity of a heating block system (HBS), a computer model was developed using finite element software COMSOL. Good agreement was obtained between the simulated and experimental block surface temperatures at three positions of the HBS and three heating rates. The validated computer model was further used to predict the effects of heating rates, the position of test insects and the addition of gases on the block and air temperature distributions. Simulation results showed that increasing heating rate reduced heating uniformity. The position of test insects in the treatment chamber largely affected their heating rate, with a position closer to the surface of the heat block providing a better temperature match between test insects and the HBS. When gas was added, block temperatures within the treatment chamber, particularly near the gas inlet, were influenced by gas speeds, temperatures and the gas channel design. The heating uniformity in the treatment chamber of the HBS was improved by heating the gas before adding it to the HBS, by routing the gas channel through the heating block to preheat the gas, and by using a relatively slow gas speed. The simulation results demonstrated that the validated computer model could be a reliable tool to evaluate the heating performance of the HBS for studying insect thermal death kinetics and optimize treatment conditions for the HBS when modified to include controlled atmospheres.

1. Introduction

Production in China of stored cereals and beans reached 539.3 and 17.3 million tons in 2012, respectively (National Bureau of Statistics of China [NBS], 2013). The main quality loss during storage is from damage due to insect pests. For example, the losses caused by pests in postharvest rice and wheat can be as high as 20% and 30%, respectively (FAO, 2013; FAOSTAT, 2013). Pest infestations cause reductions of product weight, quality, nutritional content and commercial value, and create a threat to consumer health. Chemical fumigations are widely used to control insects in stored products. To reduce chemical residues and environmental pollution, non-chemical thermal treatment methods, such as hot air, microwave and radio frequency (RF) heating, have been widely studied for disinfesting agricultural products (Tilley et al., 2007; Wang et al., 2010; Hansen et al., 2011; Opit et al., 2011).

Developing effective thermal treatment methods depends on the thermal death kinetics of target insects. A heating block system (HBS) has been successfully used as a unique device to determine the thermal death kinetics of many insects (Wang et al., 2002a, 2002b; Johnson et al., 2003, 2004; Hallman et al., 2005; Yan et al., 2014; Hou et al., 2015; Li et al., 2015). Thermal death results obtained with the HBS have been confirmed for navel orangeworm (*Amyelois transitella*) in walnuts (Wang et al., 2002c), yellow peach moth (*Conogethes punctiferalis*) in chestnuts (Hou et al., 2015) and cowpea weevil (*Callosobruchus maculatus*) in lentils (Jiao et al., 2012). The HBS can be programmed to simulate the heating rate of the interior of agricultural products (Wang et al., 2005) when subjected to different heating methods, such as hot air, hot water and RF treatments (Wang et al., 2006). However, variability in insect mortality using the HBS suggests that a systematic study of the

* Corresponding author. College of Mechanical and Electronic Engineering, Northwest A&F University, Yangling, Shaanxi 712100, China.
E-mail address: shaojinwang@nwsuaf.edu.cn (S. Wang).

http://dx.doi.org/10.1016/j.jspr.2015.11.003
0022-474X/

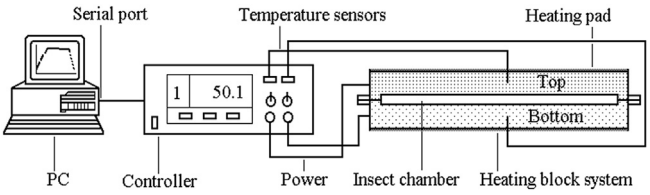

Fig. 1. Heating block system for insect mortality studies (Yin et al., 2006).

heating behaviour of the HBS with and without insects would be needed.

Controlled atmosphere (CA) treatments to control insects in agricultural products typically involve lowering O_2 and raising CO_2 concentrations (Neven and Rehfield-Ray, 2006a, 2006b; Son et al., 2012; Neven et al., 2014). The susceptibility of insects to CA increases with increasing temperature due to enhanced respiratory demand. Using heat treatments reduces the exposure time needed when using modified or controlled atmospheres (Neven and Mitcham, 1996; Shellie et al., 1997). To analyse the effects of combined heat and CA treatment on insect mortality, the HBS was modified to allow the addition of different gases (Neven et al., 2012; Li et al., 2015). However, before insect thermal death kinetic tests are determined, the effect that added gas may have on the heating rate and temperature uniformity of the HBS must be understood.

Because lengthy experimental methods to determine the effects of multiple factors are costly, computer simulation has been used to predict the effect of gas speeds and temperature on heat transfer under various conditions. Chung et al. (2008) developed a finite element model using the commercially available software FEMLAB to simulate transient heat transfer in a test cell. Tiwari et al. (2011) confirmed that non-uniform distribution of RF power density resulted in non-uniform heating in wheat flour using the finite element method. Ben-Lalli et al. (2012) defined 2D axial-symmetric domain during both convective and microwave heating treatments, and obtained 95% accuracy between the simulated temperatures and experimental data. Huang et al. (2015a) developed a 3-D theoretical model using COMSOL to determine differential heating of insects in soybeans when subjected to radio frequency treatments. Therefore, computer simulation may provide a useful tool in determining the effects of gas temperature and flow rates on the heating uniformity within the HBS.

Objectives of this study were as follows: 1) using the finite element software COMSOL, develop and validate a simulation model for the HBS under different heating rates without insects or adding gases; 2) simulate temperature differences between the aluminium block, air in the treatment chamber and test insects when test insects are placed in various positions without adding gases; and 3) apply the validated model to predict effects of different gas speeds, temperatures, and gas channel systems on temperature distribution of the HBS.

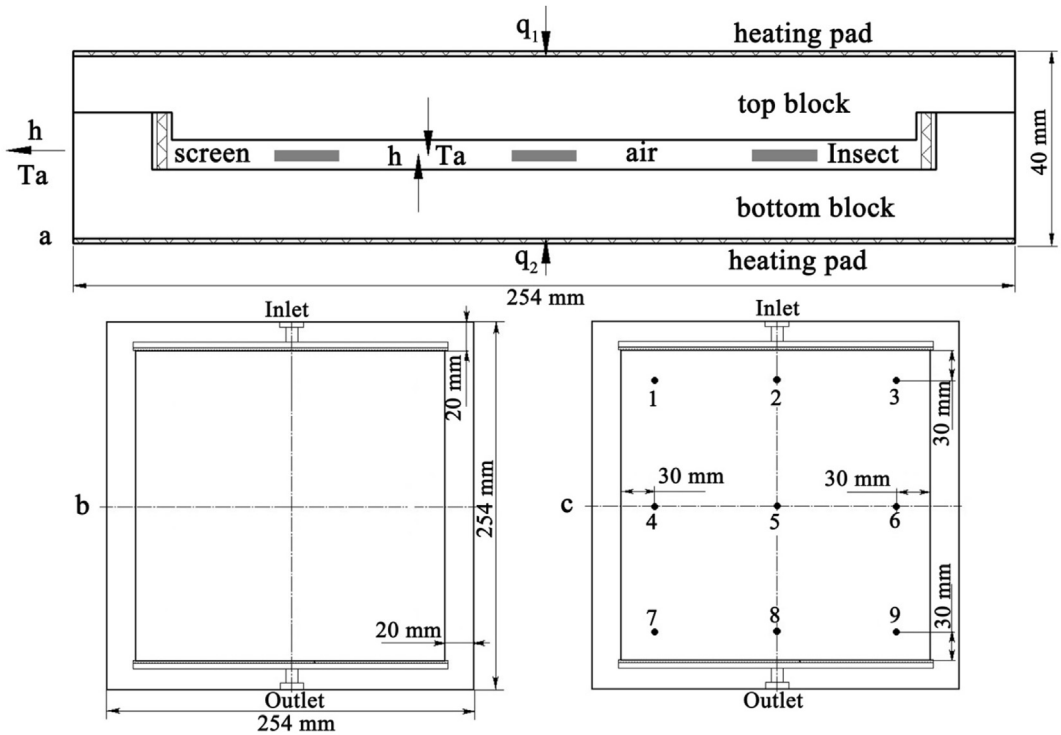

Fig. 2. Dimensions and heat transfer parameters for the model (a), dimensions of the cavity (b) used to simulate the heating block system, and positions on the bottom block surface (c) used for temperature measurement.

Table 1
Thermal properties and conditions used in the simulation (Ikediala et al., 2000).

Material	Density ρ (kg/m^3)	Specific heat c_p (J/kg°C)	Thermal conductivity k (W/m°C)
Aluminium block	2702	903	234
Insect	1036	3450	0.51
Air	1.160	1007	0.027

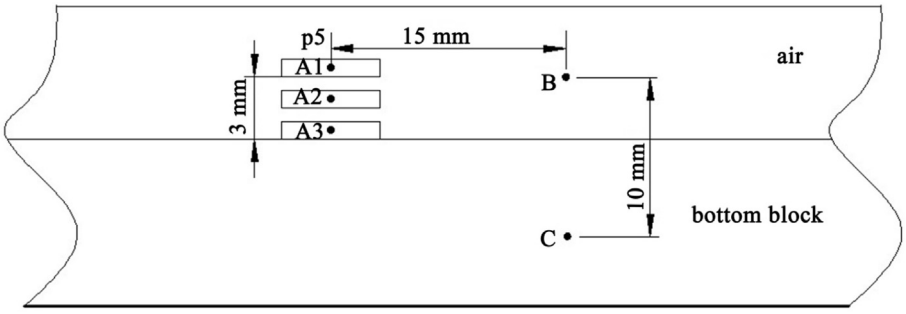

Fig. 3. Positions of simulated temperatures for pests at three heights of 3 mm (A1), 1.5 mm (A2), and 0 mm (A3) from the bottom block at the position p5, air in treatment chamber (B), and bottom block (C).

2. Materials and methods

2.1. Heating block system (HBS)

The HBS was composed of heating pads, top and bottom aluminium blocks (254 × 254 × 40 mm^3), insect treatment chamber (214 × 214 × 6 mm^3) and a data acquisition/control unit (Fig. 1). Calibrated type-T thermocouples (TMQSS-020-6, Omega Engineering Ltd., CT, USA) were used to monitor temperatures of the top and bottom blocks. Heating rates (0.1–15 °C/min) and the set-point temperature (≤60 °C) were controlled by the Visual Basic software via a solid-state relay. Two PID controllers (I32, Omega Engineering, Inc., Stamford, CT) regulated the two block surface temperatures separately. There were gas channels in the top and

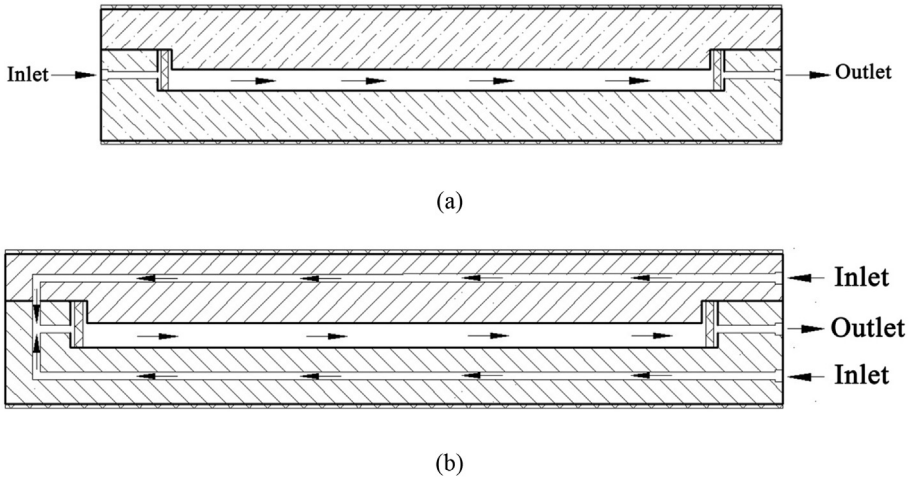

Fig. 4. Two simulated gas channel designs: short channel (a) and long channel (b).

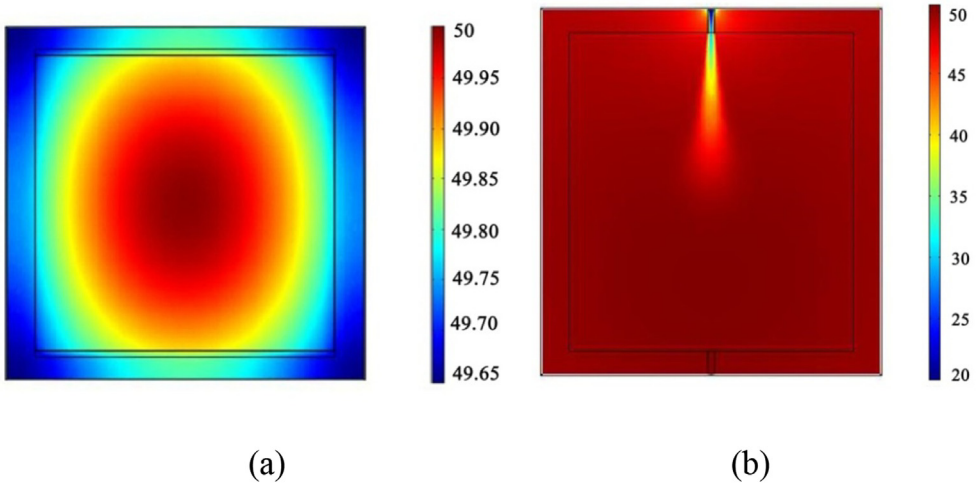

Fig. 5. Simulated temperature distributions at the horizontal section in treatment chamber of HBS when no gas was added (a) and added 20 °C gas (b) while reaching the highest temperature of 50 °C.

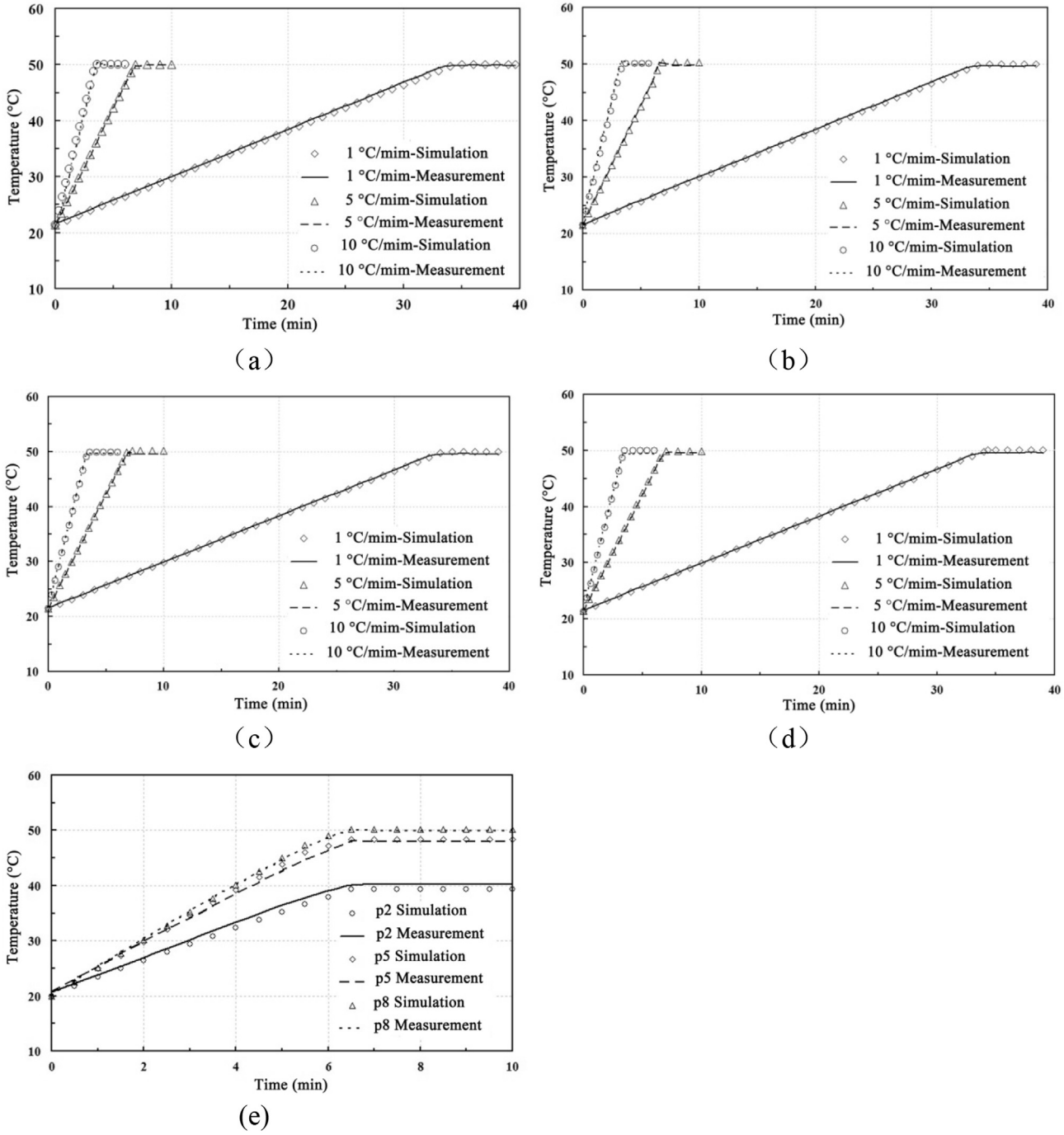

Fig. 6. Comparison of experimental and simulated temperatures over time at heating rates of 1 , 5 and 10 °C/min at p2 (a), p5 (b), and p8 (c), and the average temperatures for all positions (d) and temperatures over p2, p5, and p8 when added gas at 5 °C/min (e).

bottom aluminium blocks, which were used to add the desired controlled atmosphere (CA) to the treatment chamber. Differences in thermo-physical properties for various controlled atmospheres are slight and should have a negligible effect on the heating rate and temperature uniformity (Hilsenrath et al., 1956). Therefore, thermal properties for ambient air (21% O_2, 0.03% CO_2, and 78.97% N_2) were used in the simulation model.

2.2. Model development

2.2.1. Physical model

The HBS heat transfer model was used to simulate the temperatures of the aluminium blocks, test insects, and treatment chamber air when the heating pads were set as boundary heat sources (Fig. 2). The heat fluxes (q_1 and q_2) transferred from heating pads to top and bottom blocks and then to air and test insects through natural convection or heat conduction. The standard k-ε model was used to simulate the air turbulence in the chamber when the gas was added. The heat loss from the side walls of the heating blocks to the environment inside an insulation box was estimated by convective heat loss with h value of 5 W/m^2°C under natural convection used in the previous study (Ikediala et al., 2000).

It was assumed in the model that for temperatures of 20–50 °C, thermal properties of the aluminium block, air and insects, and

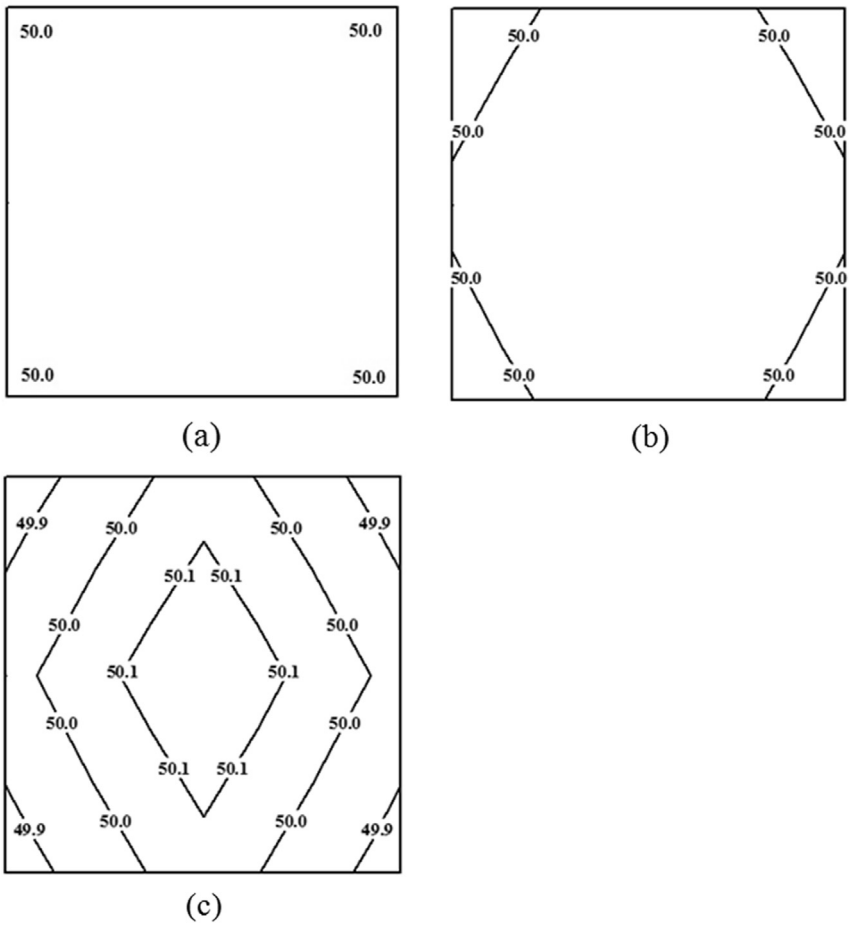

Fig. 7. Contour plot of the simulated temperature distribution in the treatment chamber when the average temperature reached 50 °C with heating rates of 0.5 °C/min (a), 5 °C/min (b) and 15 °C/min (c).

heat transfer resistances between the blocks or between heating pads and blocks were constant. Test insects were assumed to be not moving in the chamber during treatment.

2.2.2. Governing equations and boundary conditions

The heat transfer took place from the heating pads to the aluminium blocks and then to air and insects in the treatment chamber, which could be described by the following partial differential equations:

$$\rho C_p \frac{\partial T}{\partial t} = k\left(\frac{\partial^2 T}{\partial x^2} + \frac{\partial^2 T}{\partial y^2} + \frac{\partial^2 T}{\partial z^2}\right) \quad (1)$$

With the initial conditions:

$$T(x, y, z, t = 0) = T_0(x, y, z) \quad (2)$$

where ρ, C_p and k are the density (kg/m^3), specific heat capacity (J/kg°C), and thermal conductivity (W/m°C) of the material, respectively, t is the heating time (s), T is the temperature (°C), x, y, and z are the Cartesian coordinate positions (m), and T_0 is the initial temperature of the materials (20 °C). The boundary heat source q (W/m^2) transferred from the heating pad to the top or bottom block was described by Eq. (3):

$$-k\frac{\partial T}{\partial n} = q \quad (3)$$

where n is the outward normal direction to surface. Convective heat transfer between the material surface and the surrounding air was given by Eq. (4):

$$-k\frac{\partial T}{\partial n} = h(T - T_a) \quad (4)$$

where h is the surface heat transfer coefficient (W/m^2°C) and T_a is the air temperature (20 °C). Previous studies (Neven et al., 2012) used relatively low gas flow rates (4.7×10^{-4} m^3/min), with a resultant gas flow speed of about 0.006 m/s inside the treatment chamber (about 1 m/s in the gas channels). Therefore, heat transfer was assumed to be through natural convection and turbulent flow between airflow and the internal block surfaces. The h value could be calculated for plane surfaces according to the dimensional analysis as follows (Ben-Lalli et al., 2012):

$$h = 1.75(T - T_a)^{0.333} \quad (5)$$

Values for heat flux, q_1 and q_2, would vary with heating rate and block thickness, with faster heating rates or thicker blocks resulting in a larger heat flux. Therefore, the heat fluxes were calculated by the following:

$$q_i = k'\rho C_p d_i \quad (i = 1, 2) \quad (6)$$

where k' is the heating rate (°C/min), and d_1 and d_2 are the thickness of the top (17 mm) and bottom block (14 mm), respectively. Thermal properties and heat transfer parameters of aluminium, test insects and air in the simulation model are listed in Table 1 (Ikediala et al., 2000).

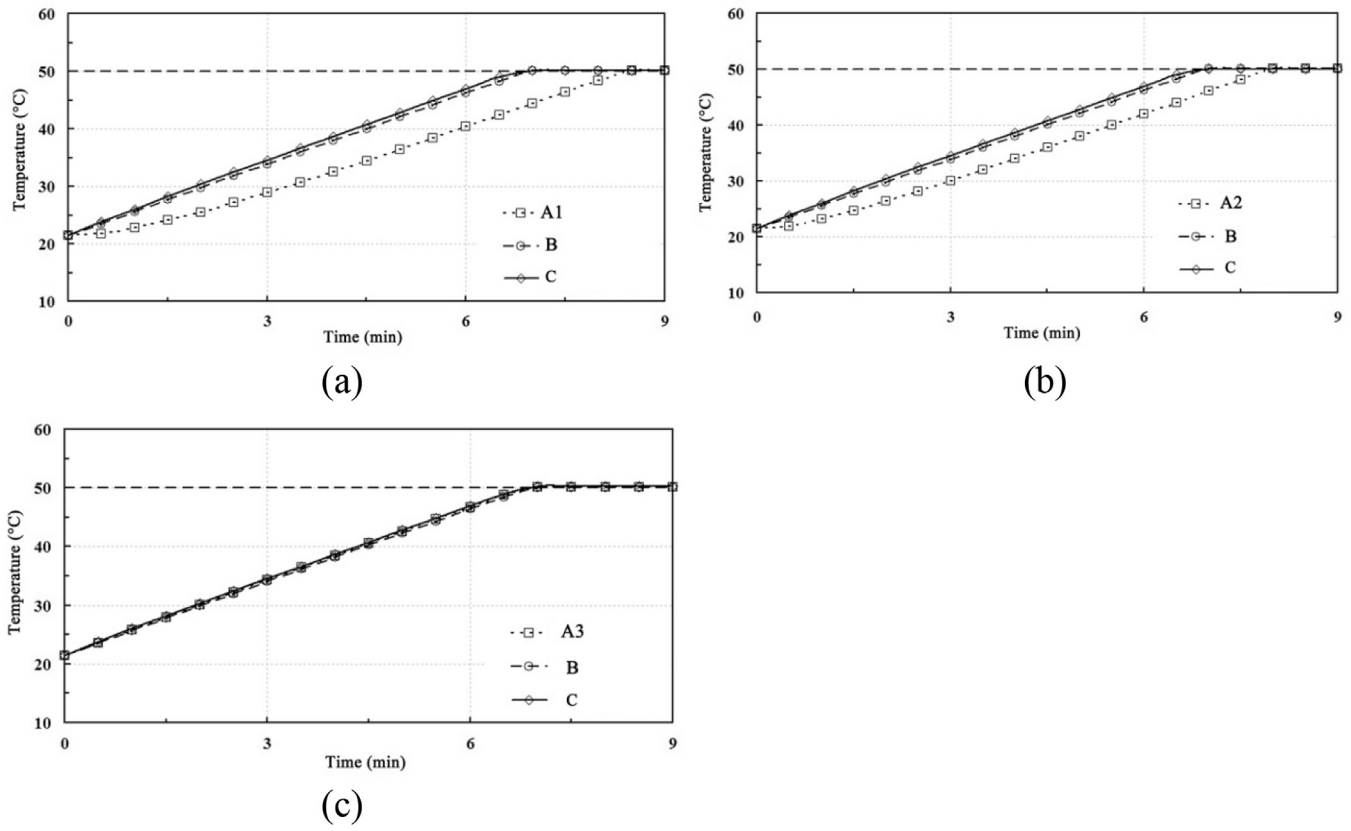

Fig. 8. Simulated temperatures for test insects with three heights of 3 mm A1, 1.5 mm (A2), and 0 mm (A3), air in the treatment chamber (B) and the heating block (C) at position 5 and a heating rate of 5 °C/min.

2.2.3. Solution methodology

A finite element method was used to solve the energy, momentum and transport equations using COMSOL Multiphysics software (V4.3a Cn Tech Co., LTD., Wuhan, China). The general steps of finite element simulation include creating 3D geometry, specifying multi-physics model, assigning initial and boundary conditions, creating and optimizing meshing, selecting solver according to the tolerance, and solving and outputting results (Huang et al., 2015b). A relatively fine tetrahedral mesh was created to solve temperature and velocity values. The mesh size was considered suitable when the temperature difference at the same point between two sequential sets of meshes was less than 1%. The final mesh system consisted of about 728,518 domain elements (tetrahedral), 127,142 boundary elements (triangular), 2935 edge elements (linear), and 53 vertex elements. Extremely fine tetrahedral mesh was generated in the food sample to guarantee the accuracy of temperature and airflow distribution results. Mesh size was chosen based on the convergence study when the difference in the resulted temperatures between successive calculations was less than 0.1%. Initial and maximum time steps for data output were set as 0.001 and 1 s, respectively. The software was run on a Dell workstation with two Dual Core 3.10 GHz Xeon processors, 8 GB RAM on a Windows 7 64 bit operating system. Each simulation task took about 10–60 min to complete, depending on the specific conditions.

2.3. Model validation

To compare measured and simulated temperatures, nine representative positions on the bottom block surface (Fig. 2) were selected for measurement at heating rates of 1, 5, and 10 °C/min based on the symmetrical temperature distribution of the HBS. Measured and simulated temperatures at p2, p5 and p8 at a heating rate of 5 °C/min were also compared when gas was added at a speed of 1 m/s. An initial heat block temperature of 20 °C was used in all tests. Surface thermocouples (SA1-T, Omega Engineering Ltd, CT, USA) and a data acquisition system (CR-1000, Campbell Scientific. Inc, Logan, Utah, USA) were used for temperature measurements.

Table 2
The maximum difference in time (s) to reach 50 °C and maximum temperature difference (°C) at 50 °C among test insect (A1, A2, and A3), air in the treatment chamber (B) and the heating block (C), (A1, A2, A3, B and C shown in Fig. 3).

Heating time and temperature difference		Distance between the bottom block and the treated pests (mm)		
		3 (A1)	1.5 (A2)	0 (A3)
Largest difference of heating time (s)	Aluminium block and air	<10	<10	<5
	Aluminium block and test insects	>150	>85	<10
Largest difference of temperature (°C)	Aluminium block and air	0.74	0.72	0.71
	Aluminium block and test insects	10.20	5.95	0.73

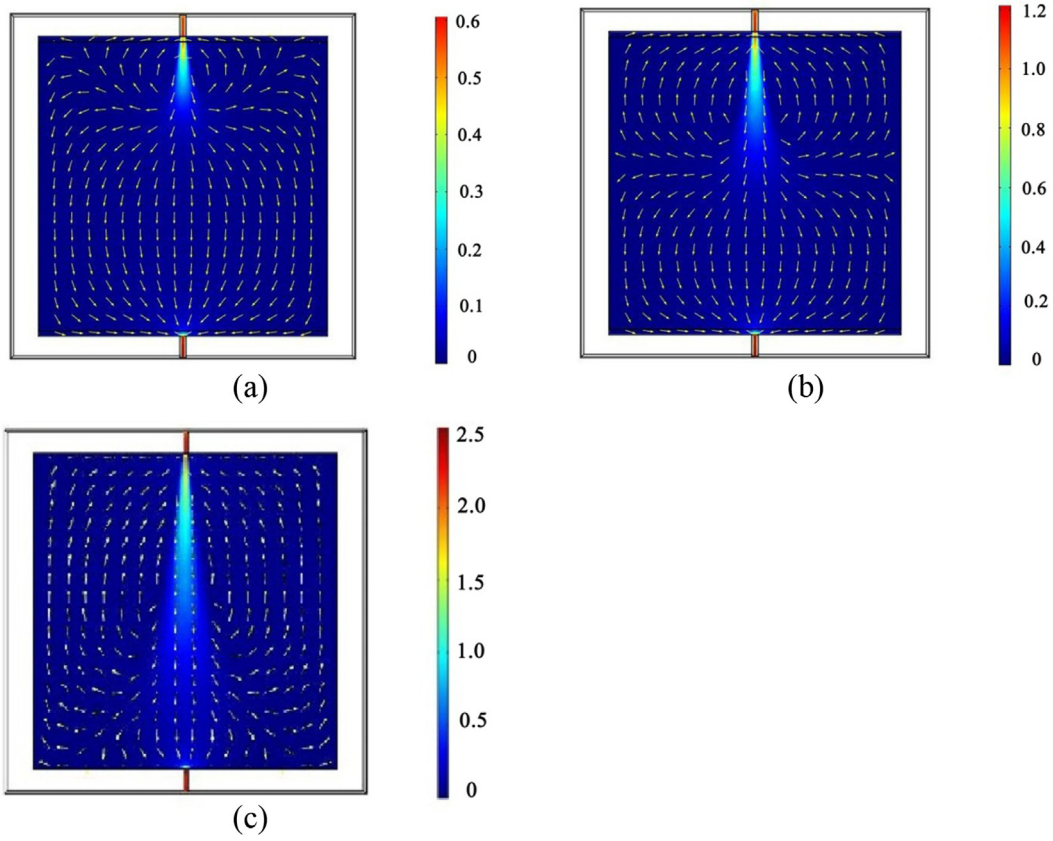

Fig. 9. Simulated gas flow fields in the treatment chamber at gas speeds of 0.5 m/s (a), 1 m/s (b) and 2 m/s (c) with short channel design.

2.4. Model predictions

2.4.1. Effect of heating rates on uniformity of the HBS

Heating rates have a significant influence on the mortality of treated pests mainly due to the difference in ramping time (Neven, 1998; Wang et al., 2002a). Heating rates of 0.5, 5 and 15 °C/min were selected for this study. The effect of different HBS heating rates to a set point of 50 °C on temperature distribution were simulated assuming no test insects or added gases.

2.4.2. Effect of test insects on heating uniformity of the HBS

In previous studies, last-instar larvae of target insects, such as Indianmeal moth, red flour beetle, rice weevil and maize weevil have been placed directly on the bottom block for thermal death kinetic studies (Johnson et al., 2003, 2004; Li et al., 2015; Yan et al., 2014). However, for eggs on wax paper sheets (Wang et al., 2004) or small rice weevil adults in nylon-mesh-screen bags (Yan et al., 2014), these insects are often suspended in the insect chamber of HBS during heat treatment. To examine the effect of position on insect heating uniformity, temperatures were simulated for treatment chamber air, the heating block, and Indianmeal moth larvae at the centre of the block (p5, Fig. 2c) at 0, 1.5 and 3 mm from the bottom block using a heating rate of 5 °C/min. A cylindrical 5th instar Indianmeal moth larva 13 mm long and 2 mm diameter, with thermal properties listed in Table 1 was assumed in the simulation model. The details of the insect and simulated temperature locations were shown in Fig. 3.

2.4.3. Effect of adding gas on the heating uniformity of HBS

Gas speed and temperature may influence heating stability and uniformity in the HBS, resulting in variations in pest mortality. Earlier CA disinfestation studies used gas speeds of 1.2–2 m/s (Neven and Rehfield-Ray, 2006b) while Neven et al. (2012) used gas speeds of 0.47 L/min (≈1 m/s) in a HBS similar to that used in the current study. Consequently, gas speeds of 0.5, 1 and 2 m/s were selected for simulations that included an initial gas temperature of 20 °C with the short channel design at a heating rate of 5 °C/min (Fig. 4a). In separate simulations, the effect of different gas temperatures (25, 35 and 45 °C) was examined under conditions of a 1 m/s gas speed and a 5 °C/min heating rate. Both simulations specifically examined the effect on the heating uniformity of inlet (p2), centre (p5) and outlet (p8) areas.

Gas channels were added to the HBS to study high temperature CA treatments. The effect of two different gas channel designs on heating uniformity was compared with and without added gas. The first design used a short gas channel through the sidewall of the block that fed the gas directly through to the treatment chamber (Fig. 4a) and did not allow pre-heating of the gas. The second used two longer gas channels through each heating block, which allowed pre-heating of the gas before it entered the treatment chamber (Fig. 4b). Because of the symmetrical structure of the HBS, the added gas should primarily affect the middle of the treatment chamber from inlet to outlet. Therefore, simulated temperatures at p2, p5 and p8 (Fig. 2c) were compared, assuming a gas speed of 1 m/s in the gas channels and a heating rate of 5 °C/min with a 20 °C initial temperature.

3. Results and discussions

3.1. Model validation

Fig. 5a shows the simulated temperature distribution in the HBS treatment chamber when the maximum temperature reached 50 °C, which confirmed the assumption of a symmetrical

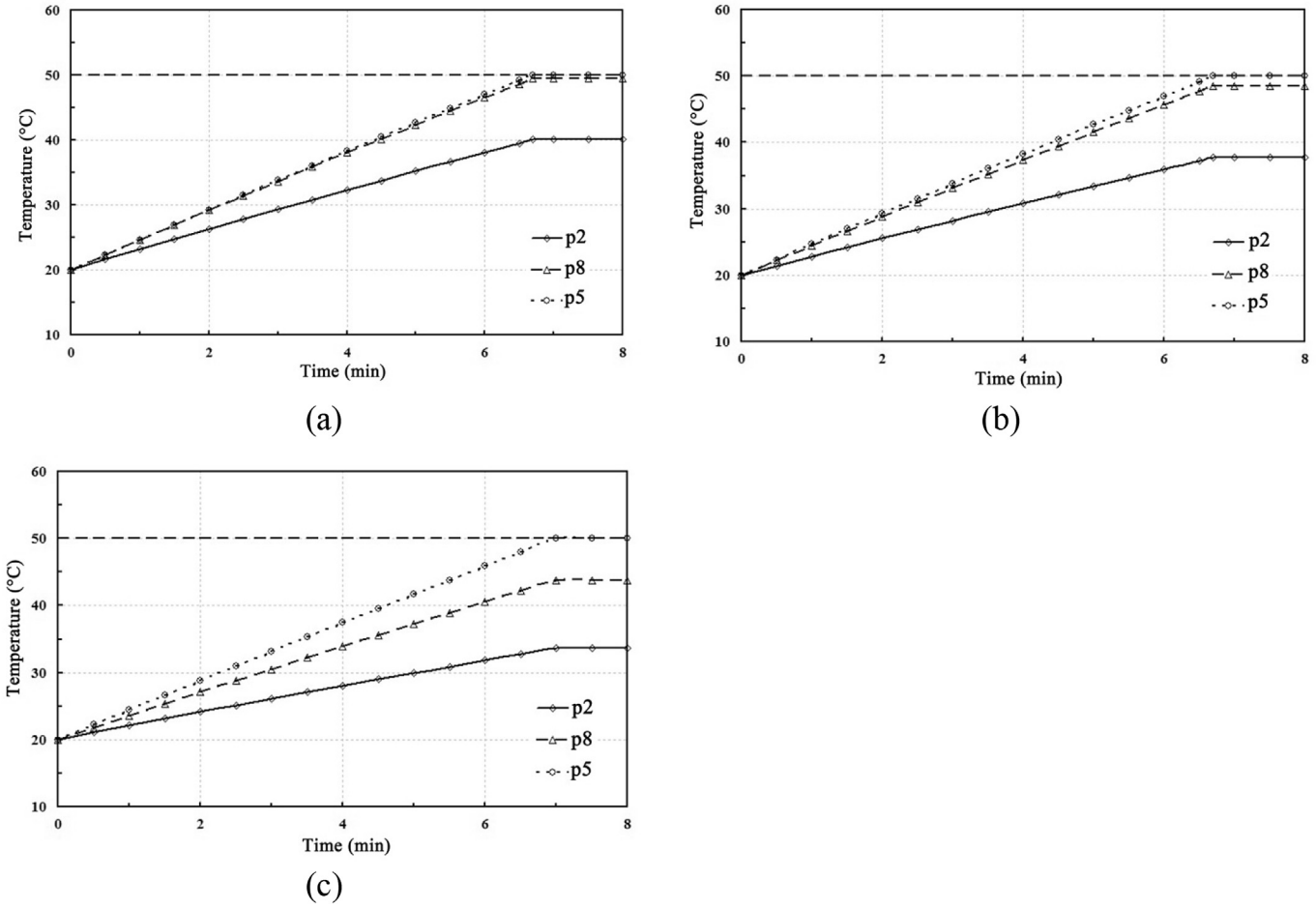

Fig. 10. Simulated temperature–time histories of positions of p2, p5 and p8 at gas speeds of 0.5 m/s (a), 1 m/s (b) and 2 m/s (c) with no gas pre-heating (short channel design).

Table 3
Temperature differences (°C) between p2 (inlet), p5 (center of the chamber) and p8 (outlet) when outlet temperature get 50 °C at gas speeds of 0.5, 1 and 2 m/s using the short-channel design and a starting gas temperature of 20 °C.

Gas speed (m/s)	p2 and p5 (°C)	p5 and p8 (°C)	p2 and p8 (°C)
0.5	9.38	0.57	9.95
1	10.80	1.48	12.28
2	10.13	6.26	16.39

temperature distribution over the central axis of the HBS. The highest temperatures were located at the centre of the HBS due to convective heat losses to the surrounding ambient air through the sidewalls of the heating block. Fig. 5b shows the simulated temperature distribution in the HBS treatment chamber when room air was directly introduced into the treatment chamber through the short channel design and the maximum temperature reached 50 °C. Only the temperature in a narrow area between the gas inlet and centre of the block was affected.

Fig. 6 compares simulated and measured temperatures over time from 20 to 50 °C. For heating rates of 1 °C/min, 5 °C/min, and 10 °C/min, simulated temperatures at p2 (Fig. 6a), p5 (Fig. 6b) and p8 (Fig. 6c) agreed well with measurements made at the same points. Average temperatures over all 9 positions (Fig. 6d) also agreed well with measurements with almost no difference in average temperatures between simulated and measured temperatures. When gas was added to the HBS at a heating rate of 5 °C/min, the simulated and experimental temperatures at p2, p5 and p8 had no obvious differences (Fig. 6e). This suggests that the assumptions, boundary conditions, and model parameters adequately represented actual heat transfer within the HBS, and the validated model could be used to simulate temperature distributions when controlled atmosphere or test insects were added to the HBS.

3.2. Effect of heating rates on uniformity of HBS

Fig. 7 shows the simulated horizontal temperature distribution of the treatment chamber at a heating rate of 0.5 °C/min (Fig. 7a), 5 °C/min (Fig. 7b) and 15 °C/min (Fig. 7c) when the average temperature reached the set-point of 50 °C. The simulated surface temperature revealed that centre temperatures were higher than temperatures in the corners or edges due to heat loss at the boundary sidewalls. Temperature uniformity decreased with increasing heating rates; the average difference between simulated temperatures and the set point (50 °C) was 0.014, 0.034 and 0.110 °C at heating rates of 0.5, 5 and 15 °C/min, respectively. A similar effect of heating rate on heating uniformity was also reported by Evans (1986), Neven (1998) and Wang et al. (2002a).

3.3. Effect of test insects on heating uniformity of HBS

Fig. 8 shows the simulated temperatures of test insects (A1, A2, and A3), air in the treatment chamber (B) and the heat block (C) when insects were located at heights of 3 mm (Fig. 8a), 1.5 mm (Fig. 8b), or 0 mm (Fig. 8c) above the bottom block in the centre

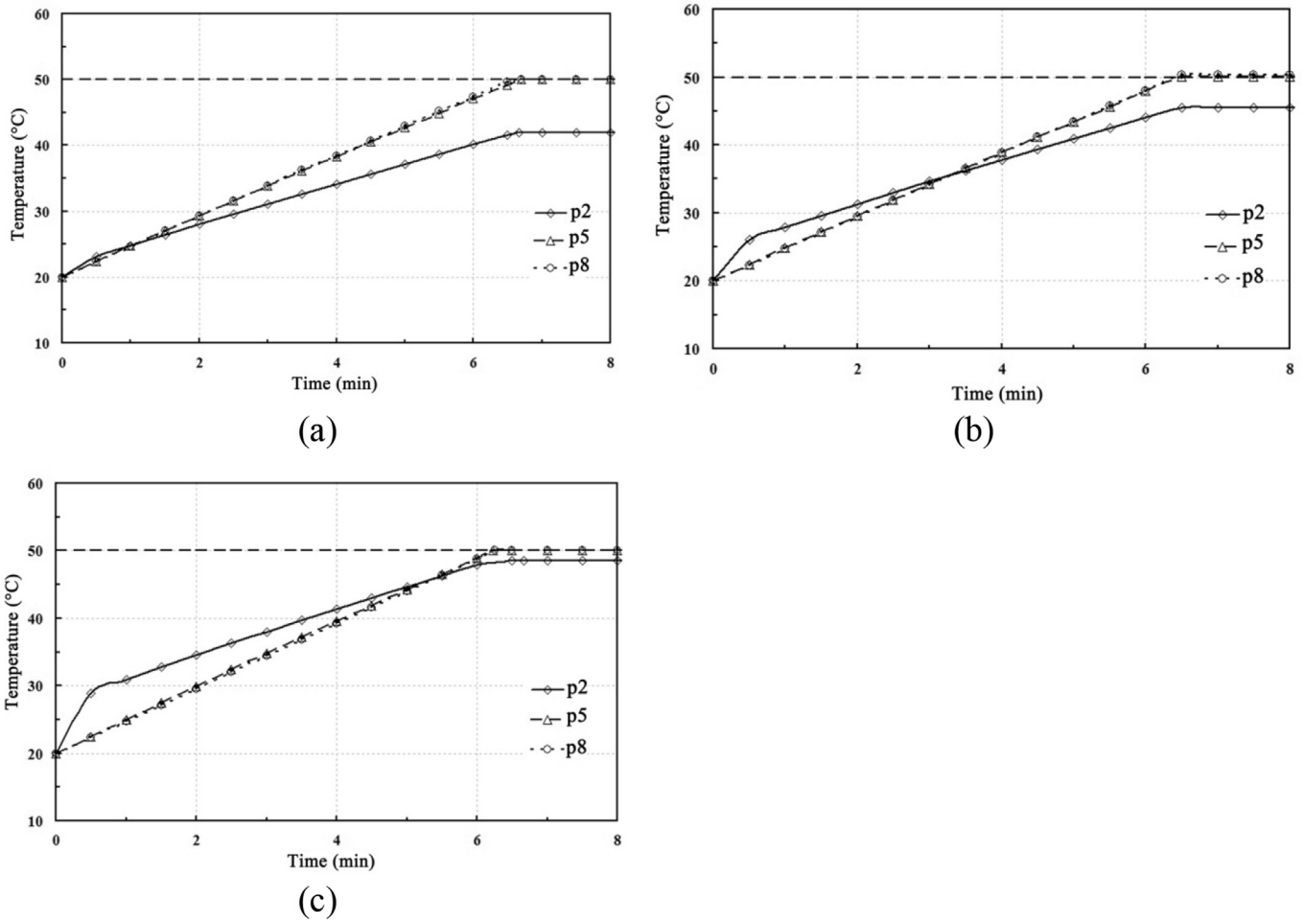

Fig. 11. Simulated temperatures over time at p2 (inlet), p5 (centre of the chamber) and p8 (outlet) at gas temperatures of 25 °C (a), 35 °C (b) and 45 °C (c) using the short channel design.

(p5) of the treatment chamber. The temperatures and heating rates of the aluminium block and the air in the treatment chamber were similar, with a small difference in the time to reach the set point. The positions of the test insect had little effect on the difference between block and surrounding air temperatures. Test insect temperatures increased more slowly when compared to the air and block temperatures, especially when insects were at heights of 3 mm (A1) and 1.5 mm (A2) from the bottom block (Fig. 8a and b). When the insects were suspended at the height of 3 mm (A1), the temperature difference between test insects and blocks was 10.2 °C, and insects took 150 s more to reach the set-point of 50 °C (Table 2). When test insects were in contact with the block surface (Fig. 8c), temperatures for insects (A3) closely followed those of the blocks, and the time and temperature differences were reduced to <10 s and 0.73 °C, respectively (Table 2). The results suggest that test insects should be in direct contact with the heat blocks during insect thermal death kinetic studies.

3.4. Effect of added gas on the heating uniformity of HBS

3.4.1. Effect of gas speed

Fig. 9 shows the simulated gas flow patterns in the treatment chamber at inlet gas speeds of 0.5 m/s (Fig. 9a), 1 m/s (Fig. 9b) and 2 m/s (Fig. 9c). Increasing gas speeds changed the gas flow patterns. Due to the small cross-section of the outlet, at higher speeds the gas flow turns back towards the inlet area once it reaches the far wall of the chamber.

As shown in Fig. 10, the heating rates of the inlet and centre of the chamber decreased with increasing gas speed for a shorter heating time. Heating rates at the inlet was lower than at the centre of the chamber or the outlet, and was caused by the constant addition of unheated gas. Due to incoming gas being heated by the time it reached the back of the chamber, gas speed had little effect on the temperature of the outlet area, although the heating rate was slightly slower at 2 m/s (Fig. 10c).

Table 3 shows the temperature differences for p2, p5 and p8 at gas speeds of 0.5, 1 and 2 m/s using the short channel design and a starting gas temperature of 20 °C. The temperature difference between p2, p5 and p8 increased with increasing gas speed. Temperatures within the treatment chamber at 0.5 m/s were more uniform than at 1 or 2 m/s, suggesting that a relative slow gas speed when adding CA to the HBS would improve the temperature uniformity of the treatment chamber.

3.4.2. Different gas temperature

As shown in Fig. 11, adding unheated (20 °C) gas to the treatment chamber had a large effect on temperature uniformity, especially at the inlet, which may affect the mortality of test insects. When the temperature of the added gas was increased, the initial temperature at the inlet was higher than that at the centre of the chamber and the outlet (Fig. 11). Temperature differences between inlet and outlet decreased with increasing gas temperature.

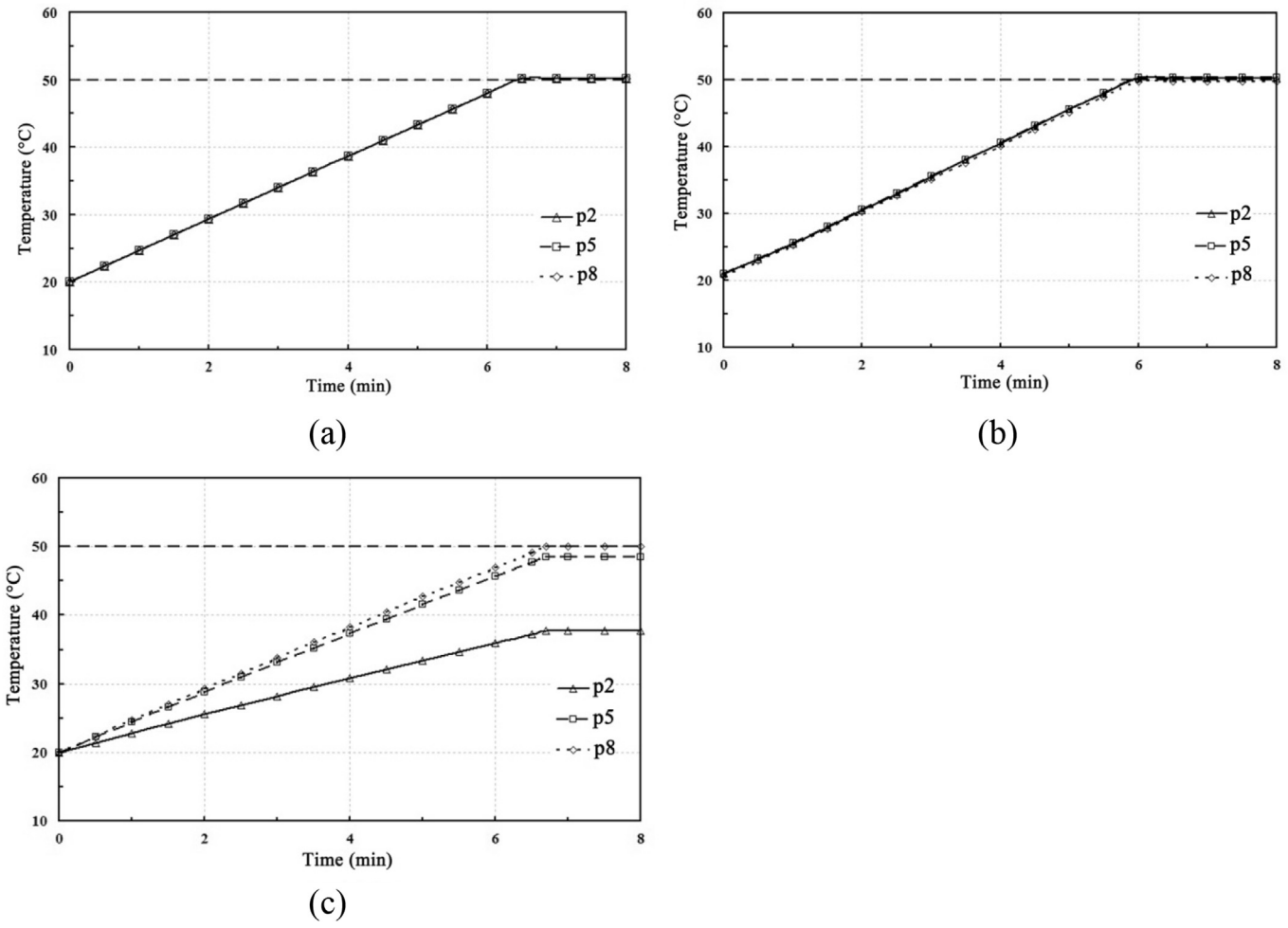

Fig. 12. Simulated temperature over time near the gas inlet (p2), centre of the block (p5) and gas outlet (p8) when no gas was added (a), gas was added by the long channel design (b) and gas was added by the short channel design (c) at 20 °C and a speed of 1 m/s.

Temperature differences were about 8.06, 4.74 and 1.50 °C when the added gas temperature was 25 °C (Fig. 11a), 35 °C (Fig. 11b), and 45 °C (Fig. 11c), respectively. When 45 °C air was added the heating rate was higher than for 25 and 35 °C air due to the higher initial temperature. Therefore, preheating the added gas at or near treatment temperatures would improve the temperature uniformity and heating rate of the HBS treatment chamber.

3.4.3. *Effect of gas channel designs*

The effects of gas channel designs on the temperatures at inlet, centre and outlet areas are shown in Fig. 12. As shown in Fig. 12a, temperature uniformity between p2, p5 and p8 was optimal for either gas channel design when no gas was added. The long channel design had a faster heating rate than either the short channel design or when no gas was added because the gas was preheated as it passed through the channel in the heat block. The temperature differences between the three points were negligible for the long channel design (Fig. 12b). The short channel design had larger temperature differences between the three points, indicating lower temperature uniformity. In particular, the inlet temperature never reached 50 °C due to the constant addition of the cooler gas. However, due to the air being heated as it travelled through the chamber, the temperature of the centre point was only slightly lower than the temperature of the outlet (Fig. 12c). Therefore, the results showed that the long channel design had a better heating rate and temperature uniformity than the short channel design.

4. Conclusions

The simulated temperatures derived from the computer model developed in this study coincided well with experimental temperatures measured at different heating rates. Simulations showed how changes in experimental design could improve the performance of the HBS. More accurate and uniform treatment temperatures would be applied by keeping test insects in direct contact with the heating block surface and near the centre of the treatment chamber. Pre-heating the added gas by running the gas channel through the heating block using relatively slow heating rates and gas speeds would improve the overall temperature uniformity in the treatment chamber. The optimized operational parameters obtained from this simulation study could be further used to evaluate insect thermal death kinetics under combined heat and CA treatments.

Acknowledgements

This research was supported by research grants from Ph.D. Programs Foundation of Ministry of Education of China (20120204110022) and General Program of National Natural Science Foundation in China (No. 31371853).

References

Ben-Lalli, A., Bohuon, P., Collignan, A., Méot, J.M., 2012. Modelling heat transfer for disinfestation and control of insects (larvae and eggs) in date fruits. J. Food Eng. 2 (116), 505–514.

Chung, H.J., Birla, S., Tang, J., 2008. Performance evaluation of aluminium test cell designed for determining the heat resistance of bacterial spores in foods. LWT Food Sci. Technol. 41 (8), 1351–1359.

Evans, D.E., 1986. The influence of rate of heating on the mortality of *Rhyzopertha dominica* (L.) (Coleoptera: Bostrychidae). J. Stored Prod. Res. 23, 73–77.

FAO, 2013. Food and Agriculture Organization of the United Nations. FAO Statistical Yearbook: World Food and Agriculture. United Nations, Rome, Italy.

FAOSTAT, 2013. Food and Agriculture Organization. Available at: http://www.stats.gov.cn/tjsj/ndsj/2013/indexch.htm.

Hallman, G.J., Wang, S., Tang, J., 2005. Reaction orders for thermal mortality of third-instar Mexican fruit fly (Diptera: Tephritidae). J. Econ. Entomol. 98 (6), 1905–1910.

Hansen, J.D., Johnson, J.A., Winter, D.A., 2011. History and use of heat in pest control: a review. Int. J. Pest Manag. 57 (4), 267–289.

Hilsenrath, J., Beckett, C.W., Benedict, W.S., Fano, L., Hoge, H.J., Masi, J.F., Nuttall, R.L., Touloukian, Y.S., Woolley, H.W., King, C., 1956. Tables of thermal properties of gases. J. Electrochem. Soc. 103 (5), 124–124.

Hou, L., Hou, J., Li, Z., Johnson, J.A., Wang, S., 2015. Validation of radio frequency treatments as alternative non-chemical methods for disinfesting chestnuts. J. Stored Prod. Res. 63C, 75–79.

Huang, Z., Chen, L., Wang, S., 2015a. Computer simulation of radio frequency selective heating of insects in soybeans. Int. J. Heat Mass Transf. 90C, 406–417.

Huang, Z., Zhu, H., Yan, R., Wang, S., 2015b. Simulation and prediction of radio frequency heating in dried soybeans for thermal disinfestations. Biosyst. Eng. 129, 34–47.

Ikediala, J., Tang, J., Wig, T., 2000. A heating block system for studying thermal death kinetics of insect pests. Trans. ASAE 43 (2), 351–358.

Jiao, S., Tang, J., Johnson, J.A., Wang, S., 2012. Industrial-scale radio frequency treatments for insect control in lentils. J. Stored Prod. Res. 48, 143–148.

Johnson, J.A., Wang, S., Tang, J., 2003. Thermal death kinetics of fifth-instar *Plodia interpunctella* (Lepidoptera: Pyralidae). J. Econ. Entomol. 96 (2), 519–524.

Johnson, J., Valero, K., Wang, S., Tang, J., 2004. Thermal death kinetics of red flour beetle (Coleoptera: Tenebrionidae). J. Econ. Entomol. 97 (6), 1868–1873.

Li, W., Yan, R., Wang, K., Chen, L., Johnson, J.A., Wang, S., 2015. Tolerance of *Sitophilus zeamais* (Coleoptera: Curculionidae) to heated and controlled atmospheres treatments. J. Stored Prod. Res. 62C, 52–57.

NBS (National Bureau of Statistics of China), 2013. Statistical Yearbook of China. China Statistical Publishing House, pp. 13–15.

Neven, L.G., 1998. Effects of heating rate on the mortality of fifth-instar codling moth (Lepidoptera: Tortricidae). J. Econ. Entomol. 91 (1), 297–301.

Neven, L.G., Mitcham, E.J., 1996. CATTS (Controlled Atmosphere/Temperature Treatment System): a novel tool for the development of quarantine treatments. J. Am. Entomol. 42 (4), 56–59.

Neven, L.G., Rehfield-Ray, L., 2006a. Combined heat and controlled atmosphere quarantine treatments for control of western cherry fruit fly in sweet cherries. J. Econ. Entomol. 99 (3), 658–663.

Neven, L.G., Rehfield-Ray, L.M., 2006b. Confirmation and efficacy tests against codling moth and oriental fruit moth in apples using combination heat and controlled atmosphere treatments. J. Econ. Entomol. 99 (5), 1620–1627.

Neven, L.G., Wang, S., Tang, J., 2012. An improved system to assess insect tolerance to heated controlled atmosphere quarantine treatment. Entomol. Exp. Appl. 143 (1), 95–100.

Neven, L.G., Lehrman, N.J., Hansen, L.D., 2014. Effects of temperature and modified atmospheres on diapausing 5th instar codling moth metabolism. J. Therm. Biol. 42, 9–14.

Opit, G.P., Arthur, F.H., Bonjour, E.L., Jones, C.L., Phillips, T.W., 2011. Efficacy of heat treatment for disinfestation of concrete grain silos. J. Econ. Entomol. 104 (4), 1415–1422.

Shellie, K.C., Mangan, R.L., Ingle, S.J., 1997. Tolerance of grapefruit and Mexican fruit fly larvae to heated controlled atmosphere. Postharvest Biol. Technol. 10 (2), 179–186.

Son, Y., Chon, I., Neven, L., Kim, Y., 2012. Controlled atmosphere and temperature treatment system to disinfest fruit moth, Carposina sasakii (*Lepidoptera: Carposinidae*) on apples. J. Econ. Entomol. 105 (5), 1540–1547.

Tilley, D.R., Casada, M.E., Arthur, F.H., 2007. Heat treatment for disinfestation of empty grain storage bins. J. Stored Prod. Res. 43 (3), 221–228.

Tiwari, G., Wang, S., Tang, J., Birla, S., 2011. Computer simulation model development and validation for radio frequency (RF) heating of dry food materials. J. Food Eng. 105 (1), 48–55.

Wang, S., Birla, S.L., Tang, J., Hansen, J.D., 2006. Postharvest treatment to control codling moth in fresh apples using water assisted radio frequency heating. Postharvest Biol. Technol. 40 (1), 89–96.

Wang, S., Ikediala, J.N., Tang, J., Hansen, J.D., 2002a. Thermal death kinetics and heating rate effects for fifth-instar codling moths (*Cydia pomonella* (L.)). J. Stored Prod. Res. 38 (5), 441–453.

Wang, S., Johnson, J.A., Tang, J., Yin, X., 2005. Heating condition effects on thermal resistance of fifth-instar navel orangeworm (*Lepidoptera: Pyralidae*). J. Stored Prod. Res. 41 (4), 469–478.

Wang, S., Yin, X., Tang, J., Hansen, J., 2004. Thermal resistance of different life stages of codling moth (Lepidoptera: Tortricidae). J. Stored Prod. Res. 40 (5), 565–574.

Wang, S., Tang, J., Johnson, J.A., Hansen, J.D., 2002b. Thermal death kinetics of fifth-instar navel orangeworms (Lepidoptera: Pyralidae). J. Stored Prod. Res. 38 (5), 427–440.

Wang, S., Tang, J., Johnson, J.A., Mitcham, E., Hansen, J.D., Cavalieri, R.P., et al., 2002c. Process protocols based on radio frequency energy to control field and storage pests in in-shell walnuts. Postharvest Biol. Technol. 26 (3), 265–273.

Wang, S., Tiwari, G., Jiao, S., Johnson, J.A., Tang, J., 2010. Developing postharvest disinfestation treatments for legumes using radio frequency energy. Biosyst. Eng. 105 (3), 341–349.

Yan, R., Huang, Z., Zhu, H., Johnson, J.A., Wang, S., 2014. Thermal death kinetics of adult *Sitophilus oryzae*and effects of heating rate on thermotolerance. J. Stored Prod. Res. 59, 231–236.

Yin, X., Wang, S., Tang, J., Hansen, J., 2006. Thermal resistance of fifth-instar Cydia pomonella (L.) (Lepidoptera: Tortricidae) as affected by pretreatment conditioning. J. Stored Prod. Res. 42 (1), 75–85.